

Article

Dilatational and Shear Interfacial Properties of Pea Protein Isolate Systems with Transglutaminase at the Air–Water Interface

Noemi Baldino ^{*}, Olga Miletì, Mario F. O. Paleologo, Francesca R. Lupi  and Domenico Gabriele 

Department of Information, Modeling, Electronics and System Engineering (D.I.M.E.S.), University of Calabria, Via P. Bucci, Cubo 39C, I-87036 Rende, Italy; o.mileti@dimes.unical.it (O.M.); oraldo.paleologo@unical.it (M.F.O.P.); francesca.lupi@unical.it (F.R.L.); d.gabriele@unical.it (D.G.)

* Correspondence: noemi.baldino@unical.it

Abstract: In recent years, the demand for foods without animal proteins has increased, both for health and ethical reasons. Replacing animal protein in foods can result in unappealing textures, hindering consumer acceptance. In this context, interfacial properties also play a crucial role in food systems like foam or emulsions. Therefore, the interfacial rheological behavior at the air–water interface of pea protein isolate (PPI) has been investigated to understand how affects food foam production. The PPI has been studied without modification and also through enzymatic treatment with transglutaminase (TG) to understand the interfacial properties of the modified proteins. Data obtained by static measurements have shown a surface activity of PPI comparable with other vegetable proteins, while the treatment with TG does not significantly alter the surface tension value and the interfacial adsorption rate. Differences have been found in the rearrangement rate, which decreases with TG, suggesting a possible crosslinking of the pea proteins. The PPI modified with TG, studied in dynamic conditions both in dilation and shear kinematics, are less elastic than PPI that is untreated but with a higher consistency, which may lead to poor foam stability. The lower complex interfacial modulus obtained under shear conditions also suggests a low long-time stability.

Keywords: interfacial viscoelasticity; crosslinking; vegetable proteins; pea protein; enzyme



Citation: Baldino, N.; Miletì, O.; Paleologo, M.F.O.; Lupi, F.R.; Gabriele, D. Dilatational and Shear Interfacial Properties of Pea Protein Isolate Systems with Transglutaminase at the Air–Water Interface. *Macromol* **2024**, *4*, 227–239. <https://doi.org/10.3390/macromol4020012>

Academic Editor: Dimitrios Bikiaris

Received: 12 March 2024

Revised: 10 April 2024

Accepted: 15 April 2024

Published: 18 April 2024



Copyright: © 2024 by the authors. Licensee MDPI, Basel, Switzerland. This article is an open access article distributed under the terms and conditions of the Creative Commons Attribution (CC BY) license (<https://creativecommons.org/licenses/by/4.0/>).

1. Introduction

During the last few years, new dietary needs have emerged in the global population, principally due to diseases or needs and intolerances; but also in connection to religious concerns and other ethical issues [1–3]. Because of this, the attention of the food industry is focusing on satisfying these needs by designing new functional products [4,5], such as protein-based foods. Many of these are multiphase systems, like desserts, and drinks, and for this reason, their structural and textural features depend upon interfacial properties. Generally, to obtain stabilized systems, proteins are employed.

Proteins are not only an essential component of the human diet, but they are also a much-used ingredient in the food industry thanks to their capacity to stabilize emulsions or foams because of their amphiphilic nature [6,7]. While animal-derived proteins, like those from milk or eggs, have traditionally been the most common source, the focus is increasingly shifting towards vegetable alternatives. This shift is driven by an increasing number of people refusing to eat food containing animal proteins [4,8]. Pea proteins are widely used in the food industry and, at the same time, scientific research is focusing on their functional properties more than in the past [9]. Pea proteins are known to be composed of about 50% salt-soluble globulins and 25% water-soluble albumins [9,10]. More specifically, the globulins fraction consists of vicilin (7S) and legumin (11S), with a molecular weight (MW) of 160–200 kDa and 300–400 kDa, respectively [9,11,12]. The former is known to have a trimeric structure, while the latter is hexameric [13]. Compared to globulins, albumins (2S) are characterized by a lower MW of about 5–80 kDa [14]. However,

pea proteins generally have poor solubility, limiting their use in the food industry. To address this, they undergo extraction and isolation methods that modify the 11S/7S ratio and the hydrophobicity of the molecules [15,16]. Additionally, pea proteins can undergo physicochemical treatments (e.g., enzymatic modification) to improve their functionality. Studies on pea protein obtained by salt extraction, for example, have shown emulsifying properties and stability similar to egg and milk proteins [16–18]. Furthermore, pea protein isolates derived from cultivars with a lower legumin/vicilin ratio exhibit improved foaming properties [10].

Analysis of pea protein isolates' interfacial properties reveals the formation of an interconnected network at the air–water interface, even with low viscoelastic moduli [10]. Interestingly, albumin fractions within the globulins exhibit a stronger foaming capacity, likely due to their lower molecular weight and smaller size, facilitating faster adsorption at the interface over time. However, this albumin film at the interface is not strong enough, which explains the poor foam stability observed with pea protein isolate [13]. Due to the low stability at the interface of the PPI and, in general, of the other proteins at the air–water interface, surfactants, such as polyoxyethylene (20) sorbitan monolaurate (Tween 20), and also transglutaminase (TG) were studied [6,9]. It was found that Tween 20, as well as TG, improve the foam stability; the first one stabilizes foam by protein displacement while the second does so by crosslinking. Specifically, TG acts as a crosslinking catalyst, facilitating a two-step reaction. In the first step, the cysteine residue of TG, a nucleophilic active thiolate group, attacks an acyl donor, forming an intermediate thioester and releasing ammonia. Secondly, a nucleophilic attack by an amino group from a peptide-bound lysine residue in the protein (acting as an acyl acceptor) regenerates the thiolate group and forms a covalent intermolecular bond. This bond is resistant to both physical and chemical degradation agents [19]. Moreover, it also improves the interfacial layer of protein systems because it acts on the electrostatic repulsions among proteins at the air–water interface [6,20]. Consequently, the emulsifying and foaming properties of protein systems are improved by TG activity [6,21,22].

Despite extensive use of transglutaminase (TG) in the food industry [6,20,23,24] and decades of research in this area [25], its impact on interfacial properties remains largely unexplored [6]. Therefore, this study aimed to understand the interfacial rheological properties of pea protein isolate (PPI) solutions at the air–water interface. We investigated PPI solutions with and without TG treatment to assess the enzyme's effect. Interfacial rheological properties were evaluated using both dilatational and shear kinematics.

2. Materials and Methods

2.1. Samples Preparation

Commercial pea protein isolate (PPI) was purchased from Bulk Powders® (Brunel Way, Colchester, UK) with a protein purity of 80%. Twice-distilled water was provided through a Milli-Q purification system (Millipore, Molsheim, France), and the surface tension value was found to be 72.5 ± 0.5 mN/m at 20 °C. Pea protein solutions (P solution) were prepared by dissolving the real protein amount in twice-distilled water for two hours at room temperature using a magnetic stirrer (AREX Heating Magnetic Stirrer, Velp Scientifica, Usmate, Italy). The protein concentration was varied in the range between 1 and 10^{-5} w/w. After stirring, the solutions were centrifuged at 2900 rpm for 30 min (Centrifuge 5810, Eppendorf, Hamburg, Germany) to separate the residual fraction and avoid optical interference during the measurements. The supernatant liquid was used for the measurements. In particular, the solution with 1% w/w of protein is identified as P. A food enzymatic preparation ("HI-NET Supreme Q", HI-FOOD Spa, Parma, Italy) based on pure transglutaminase (TG) from *Streptomyces* was kindly supplied by HI-Food (Parma, Italy). According to the producer data sheet, the protein content is, as an average value, $15 \pm 2\%$ w/w, and the enzymatic activity is 400 U/g. The TG effect was tested by adding 0.25% w/w of TG to 1% w/w of P solution, named PTG solution [4]. PTG solution

was prepared according to the literature [6,20]. In detail, the amount of TG was added to 1% *w/w* of P solution after the centrifugation step.

The resulting solution was stirred by magnetic stirring (AREX Heating Magnetic Stirrer, Vel Scientifica, Usmate, Italy) at 40 °C for 2 h to favor the crosslinking reaction.

2.2. Measurements of ζ -Potential

PPI charge was evaluated by ζ -potential on the P solution at 1% *w/w*. The analysis was performed at different pH values varying from acid to basic conditions, following the procedure reported in the literature [26]. Measurements were carried out using a zeta potential analyzer (Zetasizer Nano ZSP, Malvern Panalytical Ltd., Worcestershire, UK). After solution preparation, as reported previously, the pH of the supernatant was adjusted at different pH values thanks to a proper amount of 6 N NaOH (Titolchimica, Pontecchio Polesine, Italy) for the basic conditions and 6 N HCl (Titolchimica, Pontecchio Polesine, Italy) for acid ones [7]. The tests were repeated three times.

2.3. Interfacial Measurements

Interfacial measurements in dilatational kinematic were performed with a Pendant Drop Tensiometer (FTA200, First Ten Angstroms, Portsmouth, NH, USA) at room temperature (22 ± 1 °C), putting the aqueous solutions to be investigated in a glass Hamilton syringe (1710TLL) of 100 mL. The syringe used for all tests was equipped with a stainless-steel needle (D = 20 gauge) and the experiments were carried out investigating solution with a predetermined volume. Static, dynamic, and transient tests were performed. Static interfacial tension measurements were performed while maintaining the drop volume constant and for a period of 2 h, following the procedure in the literature [27,28] to obtain the adsorption isotherms.

Dynamic oscillatory tests (i.e., frequency sweep test) in dilatational kinematics were performed by making a drop of the desired volume and subjecting the interfacial area to cycles of expansion and compression that follow a sinusoidal time function. The frequency range investigated was between 0.005 Hz and 0.1 Hz. The duration of each test was 30 min and the tests were performed at room temperature. Oscillating amplitude was chosen in the linear region, previously determined with amplitude oscillating tests [7].

Relaxation tests were performed by making the drop form and leaving it in static conditions for the time necessary to reach the equilibrium conditions, evaluated by the static measurement, as described above. After this equilibration time, the interfacial area underwent 4 square-wave cycles of expansion and compression, and each cycle duration was 300 s [7,29]. The square-wave amplitude was chosen out of the linear region.

Shear kinematic tests were carried out with an Interfacial Shear Rheometer ISR400 (KSV Instruments, Espoo, Finland), equipped with a magnetic needle (weight = 0.0086 g, length = 28.11 mm) [7]. The measures were performed in small-amplitude oscillation mode, in the linear region, preliminarily evaluated by an amplitude sweep test. Dynamic time sweep tests at 0.1 Hz were performed to study the aging of the interface and ensure the complete formation of the interfacial layers. Then, the frequency sweep tests were performed in the range between 0.05 Hz and 2 Hz in linear viscoelastic conditions after an aging time of the interface of 3 h. All the types of tests were repeated in triplicate.

2.4. Bulk Viscosity

To assess the impact of TG on the overall solution behavior, the steady-state viscosity of the PPI solutions was measured to understand how TG treatment might influence the resistance of the solution to flow. The tests were carried out with a rotational rheometer (MCR 702 Anton Paar, Graz, Austria) using a parallel plate geometry ($\Phi = 50$ mm; gap = 1.2 ± 0.1 mm) equipped with a Peltier system to control the temperature. The shear rate range investigated was set between 0.1–500 s^{-1} . Tests were performed on pure protein solution at a concentration of 1% *w/w* and on the solution at the same pea protein concentration added with TG. All tests were performed at 25 ± 1 °C and in triplicate.

2.5. Data Analysis

Equilibrium interfacial tension was evaluated for each pea protein concentration investigated in order to obtain the adsorption isotherm. From static interfacial tension data, kinetic parameters were obtained. According to the literature, the kinetics of proteins can be described in three main steps [7,27]: diffusion of proteins from the bulk to the interface, adsorption of the proteins at the interface, and rearrangement at the interfacial layer. The diffusion step generally follows the well-known Ward–Torday equation [30]:

$$\pi(t) = \gamma(t_0) - \gamma(t) = C_0 k_B T \left(\frac{D_{diff} t}{\Pi} \right)^{\frac{1}{2}} \quad (1)$$

where $\pi(t)$ and $\gamma(t)$ are the surface pressure and the interfacial tension at any time t respectively, $\gamma(t_0)$ is the interfacial tension at the initial time, t_0 , C_0 is the bulk concentration, k_B is the Boltzmann constant, T is the absolute temperature, D_{diff} is the diffusion coefficient and Π is the Greek symbol for Pi (approximately 3.14159). Plotting π versus $t^{1/2}$, if the process is diffusion-controlled, a linear trend is obtained, and from the slope of the curve it is possible to evaluate the diffusion rate, k_{diff} [7,31], as follows:

$$\pi = k_{diff} t^{1/2} \quad (2)$$

with

$$k_{diff} = C_0 k_B T \left(\frac{D_{diff}}{\Pi} \right)^{\frac{1}{2}} \quad (3)$$

both absorption and rearrangement steps are modelled with Graham and Philipps's equation:

$$\ln \frac{\pi_\infty - \pi(t)}{\pi_\infty - \pi_0} = -k_i t \quad (4)$$

where π_0 and π_∞ are the initial and the equilibrium surface pressure, respectively. From the plot of $\ln \frac{\pi_\infty - \pi(t)}{\pi_\infty - \pi_0}$ versus t , two different slopes can be identified, the first being related to the adsorption rate, k_{ads} , while the second is related to the rearrangement, k_{rearr} [7,31].

From dynamic interfacial dilatational tests, E'_d and E''_d moduli were obtained together with the phase angle, δ [7]. As reported in the literature, E'_d and E''_d relate to the solid and liquid behavior, respectively, and thanks to them it is possible to evaluate the complex dilatational modulus, E_d^* , according to the following relationship:

$$E_d^* = \sqrt{E_d'^2 + E_d''^2} \quad (5)$$

It is known from the literature that the trend of the complex modulus for weak interfaces can be fitted by a power law equation, as follows [7]:

$$E_d^* = k_d \cdot \omega^{n_d} \quad (6)$$

where k_d is a measurement of the interfacial strength, while n_d is related to the interfacial structuration degree [7,31].

The stress relaxation tests were interpreted by the following equation [32]:

$$\ln \frac{\pi(t) - \pi_\infty}{\pi_0 - \pi_\infty} = - \left(\frac{t}{\tau} \right)^\beta \quad (7)$$

where τ is the average relaxation time and β is a parameter indicating the spreading of relation times and it ranges between 0 and 1. In particular, $\beta = 1$ refers to a single relaxation time, while $\beta < 1$ indicates the presence of a spectrum of relaxation times [7,31].

Moreover, the dilatational effective surface elasticity, E_d , and the dilatational viscosity, η_d , were evaluated [29]:

$$E_d = \frac{\gamma_0 - \gamma_\infty}{\Delta A / A} \quad (8)$$

$$\eta_d = \frac{\gamma_0 - \gamma_\infty}{\frac{dA}{dt} / A} \quad (9)$$

In the equations above, γ_0 is the interfacial tension at the beginning of the relaxation curve, i.e., after sudden area expansion, γ_∞ is the equilibrium interfacial tension, $\Delta A / A$ is the variation of the interfacial area compared to the area before the sudden expansion, while $\frac{dA}{dt} / A$ is the velocity of interfacial area variation. From shear kinematic dynamic oscillation, the storage modulus (G') and loss modulus (G'') were evaluated as functions of frequency (ω). G' represents the elastic or solid-like behavior at the interface, while G'' reflects the viscous or liquid-like behavior. From these, the complex modulus can be obtained [7,33]:

$$G_s^*(\omega) = \sqrt{G_s'^2(\omega) + G_s''^2(\omega)} \quad (10)$$

where, as their ratio is the loss tangent:

$$\tan(\delta) = \frac{G_s''}{G_s'} \quad (11)$$

$G_s^*(\omega)$ versus ω trend was fitted by a power law equation:

$$G_s^*(\omega) = k_s \cdot \omega^{n_s} \quad (12)$$

where k_s refers to interface strength and n_s to the interfacial structuring degree [7].

The viscosity data were interpreted by the power law equation [31]:

$$\eta = k \cdot \dot{\gamma}^{n-1} \quad (13)$$

where η is the viscosity, $\dot{\gamma}$ the shear rate, k and n are the consistency index and the flow index, respectively.

The data were evaluated with a one-way analysis of variance (ANOVA) test at a 5% significance level and a Fisher test for means comparison using the software OriginPro (Version 2021b, OriginLab Corporation, Northampton, MA, USA).

3. Results and Discussion

3.1. Results of ζ -Potential Analysis

The electrophoretic analysis of PPI revealed an isoelectric point (IP) of 4.0 ± 0.1 , as shown in Figure 1. At this pH, the net charge of the protein becomes zero. This result is in line with previous findings, although with slight variations. Literature works reported an IP value of 4.3 or a pH of 4.5 for isoelectric precipitation of pea proteins [34,35]. Notably, the isoelectric point of pea protein aligns closely with other vegetable proteins like hemp, soy, and rice, which typically fall within the range of 4 to 4.5 [7,36,37].

At a pH of 7.2 ± 0.5 , all pea protein (P) solutions exhibited a zeta-potential of -25.6 ± 0.1 mV. This value aligns well with literature reporting zeta-potential values of -21.0 ± 0.26 or -20.9 ± 0.44 mV for pea protein isolate (PPI) extracted by isoelectric precipitation or salt extraction, respectively, at a pH of 7.0 [38]. Notably, these pH conditions promote good solubility, making pea protein suitable for applications in baked goods or diet drinks [35]. Moreover, the use of proteins in charge condition promotes the stability of the phenomena associated with the formation of multiphase systems useful for the formulation of some foods [39].

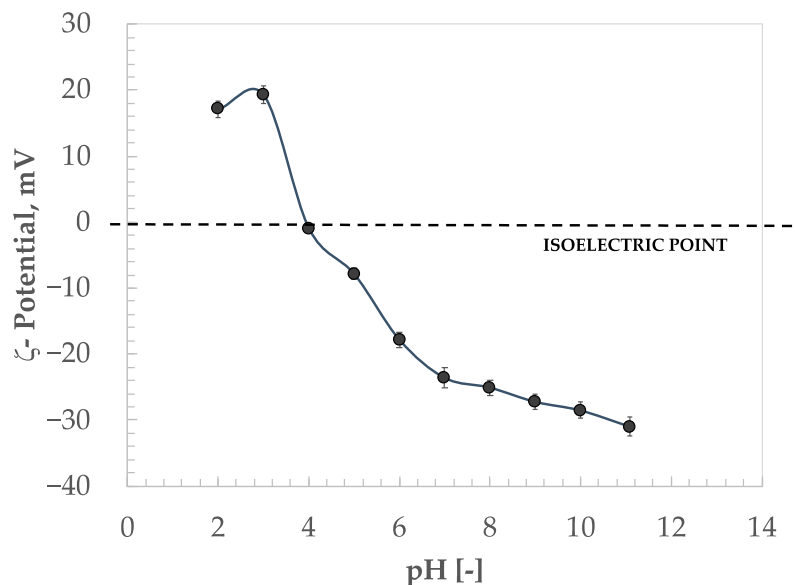


Figure 1. ζ-Potential values for the investigated PPI at different pH conditions and at 1% w/w of P solution.

3.2. Static Surface Analysis

The surface tension of PPI solutions was evaluated at several concentrations by a pendant drop tensiometer. Thanks to the surface tensions, the isotherm was obtained and the results are shown in Figure 2. The dependence of interfacial tensions in the function of the real pea protein concentration shows a sigmoidal trend, which is typical for surfactant species of the biopolymeric type but also for other vegetable proteins, such as soy, hemp and brown rice, which were already tested in previous work [7,40]. In particular, at low protein concentrations, the surface effect is absent, and the isotherms curve shows a plateau that corresponds to the ultrapure water interfacial tension of 72–73 mN/m [7]. As the concentration of pea protein isolate (PPI) increases, the equilibrium value of interfacial tension at the air–water interface decreases. At high protein levels, the equilibrium interfacial tension reaches a value of 44.6 ± 0.4 mN/m [9,13].

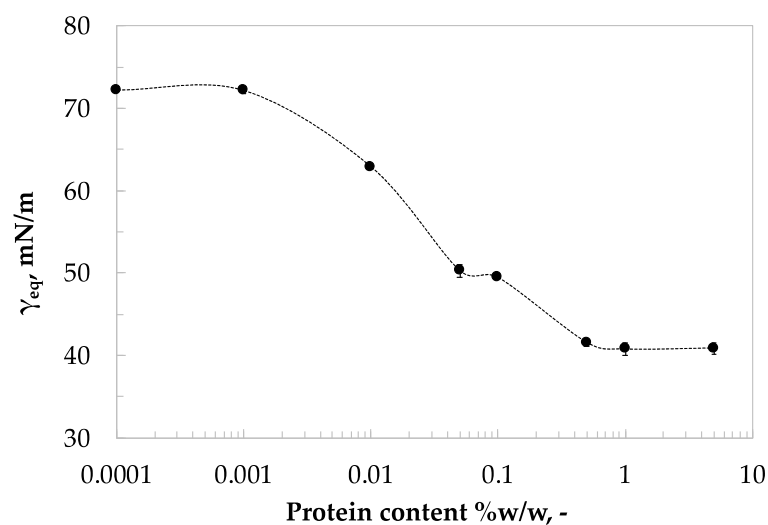


Figure 2. Equilibrium surface tension values for PPI at different concentrations.

When there is enough protein to reach the condition of the full interface coverage, the surface tension does not change despite the further increment in concentration; it is possible to observe that this situation is reached at a concentration of 1% w/w of pea protein. This

interfacial tension value is comparable with other proteins widely used in food products to stabilize the complex food system [41]. Interestingly, other vegetable proteins like soy, hemp, and brown rice also achieve complete adsorption at the air–water interface at a concentration of 1% *w/w* [7]. In particular, the surfactant effect of PPI is similar to soy proteins, which show a surface tension of 40 mN/m at saturation concentration [7]. The surfactant effect of PPI is good if compared with animal proteins such as ovalbumin or casein [27,42]. In particular, β -casein exhibits an equilibrium value of 45 mN/m, suggesting an interfacial effect similar to the PPI investigated. Notably, both proteins reach saturation at a similar concentration [42]. Also, for ovalbumin protein, the comparison with the literature showed a similar surfactant effect and a similar concentration for full surface coverage [27].

The effect of transglutaminase was evaluated at the saturation concentration, studying the P and PTG solutions. Then, the surface tension of the PTG sample was measured and the value was measured and is equal to 42.8 ± 2 mN/m, respectively, almost equal to the protein without TG. Figure 3 compares the surface tension of P and PTG samples over time. As evident from the graph, both P and PTG solutions reach very similar surface tension values, with only a slight difference. This suggests that both enzyme-treated and untreated proteins ultimately achieve a similar interfacial coverage.

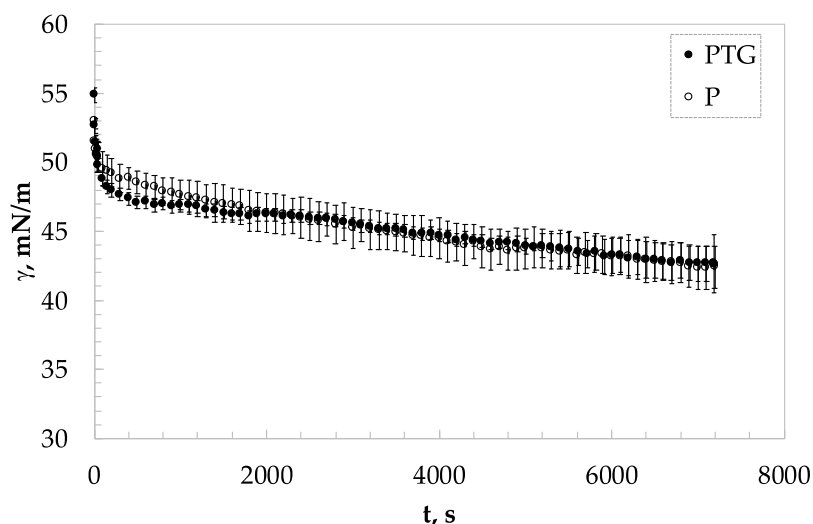


Figure 3. Surface tension of P and PTG samples.

The transient surface tension data were interpreted by the kinetic model reported in the previous section to evaluate the kinetic parameters involved in the interfacial mechanism. Typically, protein molecules in solution tend to migrate from the bulk to the interface through diffusion mechanisms, driven by the concentration gradient between the two phases. Followed by adsorption at the interface, the adsorbed protein then undergoes rearrangements to reach a more energetically favorable state, known as the rearrangement phase [27,43]. The data obtained by fitting with specific equations are reported in Table 1.

It was possible to evaluate the rates of diffusion (k_{diff}), absorption (k_{ads}), and rearrangement (k_{rearr}) from the curves and observe that as the concentration of the protein in solution increases, the diffusion rate increases [7,27]. Moreover, from the concentration value of 0.5% *w/w*, the diffusion rate is too high to be detected [44], while at low protein concentrations, the absorption and rearrangement parameters are not evaluable. However, a comparison with other previously studied vegetable proteins, such as soy, brown rice, and hemp, shows that pea protein exhibits a slower adsorption rate. It is noteworthy that the rates for all these proteins fall within a similar range [7]. In the concentration range between 0.05 and 0.5% *w/w*, the increase in the protein quantity leads to a decrease in the absorption rate at the interface, as already observed for other vegetable proteins [7], while the rearrangement phenomena become faster as the protein increases. In general, the

observed kinetic parameters for protein adsorption are consistent with those reported in the literature for interfacial active plant and animal proteins [7,40,45,46].

Table 1. Kinetic parameters for studied samples.

TG Concentration, % w/w	Protein Concentration, % w/w	k_{diff} ($m \cdot Nm^{-1} \cdot s^{-0.5}$)	$k_{ads} \cdot 10^4$ (s^{-1})	$k_{rearr} \cdot 10^4$ (s^{-1})
0	0.001	Not detectable	Not detectable	Not detectable
0	0.01	0.17 ± 0.01^a	Not detectable	Not detectable
0	0.05	0.94 ± 0.01^b	3.35 ± 0.02^a	5.69 ± 0.02^c
0	0.1	1.11 ± 0.01^c	2.50 ± 0.70^b	9.70 ± 0.70^c
0	0.5	too fast	2.11 ± 0.03^b	8.63 ± 0.04^c
0	1	too fast	2.60 ± 0.03^b	24.8 ± 0.3^a
0.25	1	too fast	2.59 ± 0.35^b	16.5 ± 1.0^b

Different letters in the same column refer to significantly different values. k_{diff} is the rate of diffusion, k_{ads} is the absorption rate and k_{rearr} is the rate of rearrangement.

The addition of TG does not change the adsorption rate but influences the rearrangement, lowering the capacity of the proteins to organize at the interface. The observed phenomena can be due to the reaction of TG with protein. The addition of TG has a direct effect on the crosslinking of amino acids present in protein fractions, as reported in the literature [20]. Then, there may be a crosslinking of amino acid fractions that can lead to the formation of higher molecular weight complexes that, due to their greater size, have less agility in molecular rearrangement phenomena at the interface [47]. Different examples of the effect of TG on protein are present in the literature [6,20,23,24].

3.3. Interfacial Dilatational and Shear Measurements

The interfacial rheological behavior of P and PTG samples was evaluated by dilatation measurements in the linearity region. The results were reported in Figure 4a,b in terms of dilatational complex modulus (E_d^*) and phase angle (δ) as a function of the frequency.

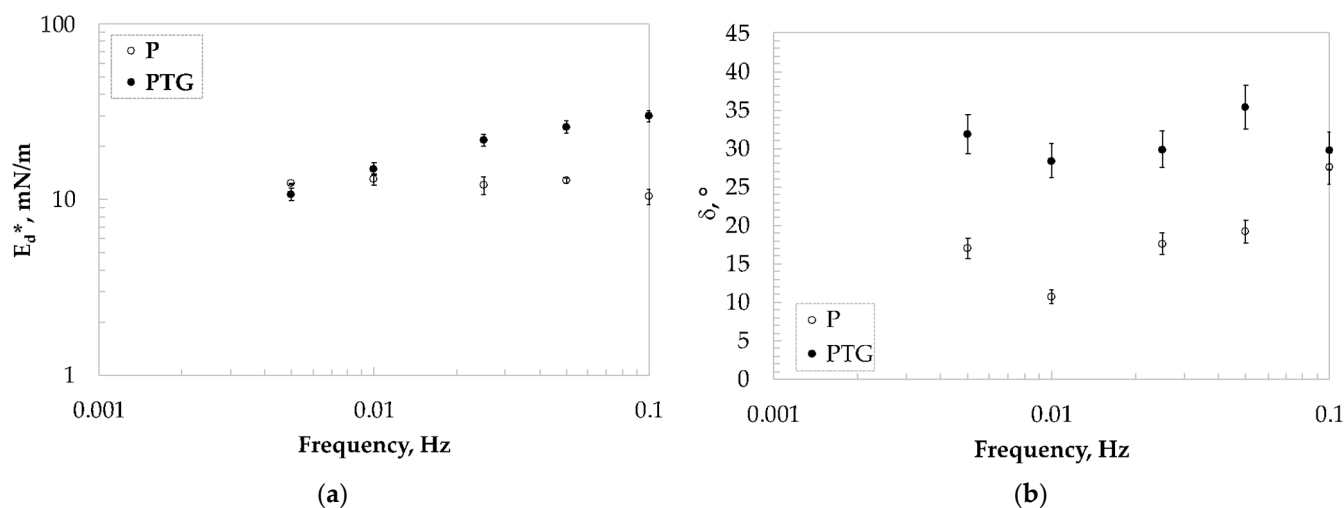


Figure 4. Surface dilatational complex modulus, E_d^* , (a) and phase angle, δ , (b) for P and PTG samples.

The frequency sweep tests show a complex modulus comparable with other food proteins such as soy and β -casein [7,40]. The frequency dependency of the P solution is low and E_d^* is almost constant with the frequency, suggesting a good structure of the interface as confirmed by the low angle phase. In fact, observing the value of the phase angle, which is about 20° , it is possible to affirm that the interface shows a solid-like and predominantly elastic behavior [10]. These results agree with similar systems found in the literature [13]. The features observed in Figure 4a suggest the formation of a well-structured

interfacial layer. Furthermore, the low phase angle indicates that the elastic modulus (E') is the dominant contributor to the complex dilatational modulus (E_d^*). In comparison, the complex dilatational modulus trend of the PTG solution exhibits a stronger frequency dependence compared to the P solution. This suggests that the enzyme treatment might influence the viscoelastic properties of the protein layer at the interface. Therefore, the addition of TG results in a weak gel behavior of the interfacial layer. The phase angle analysis still suggests a solid-like interface but with higher values than that found for the P solution. The trend can be attributed to the decrease in the protein surface hydrophobicity that causes a lower interaction at the air interface and a less structured interface [48].

The dilatational data were interpreted with the critical gel model, as mentioned in Section 2, and the results are reported in Table 2.

Table 2. Critical gel model parameters for 1% w/w protein samples, in dilatational and shear kinematics.

Sample	k_d , mN/m·s ⁿ	n_d , -	k_s , mN/m·s ⁿ	n_s , -
P	13.2 ± 0.5 ^a	0.10 ± 0.01 ^b	0.43 ± 0.02 ^a	0.12 ± 0.02 ^b
PTG	71.0 ± 3.0 ^b	0.34 ± 0.04 ^a	0.13 ± 0.06 ^b	0.66 ± 0.05 ^a

Different letters in the same column refer to significantly different values. $k_{d/s}$ is the interfacial strength in dilation or shear kinematic, $n_{d/s}$ is the interfacial structuration degree in dilation or shear kinematic.

The critical gel analysis shows the important effect of the TG on the structure of the gel. In particular, the presence of TG leads to the formation of more consistent interfaces with k_d values greater than those that characterize the interface with the protein alone. The parameter n_d , on the other hand, increasing in the presence of TG, detects a less elastic structure compared with the solution P. Comparing these results with those obtained for soy proteins [7] reveals that the interfacial film strength and elasticity (as indicated by E') of pea protein films are lower, but within a comparable range. This suggests that pea proteins have the potential for various food applications similar to those of soy proteins.

Stress relaxation tests were performed on the P and PTG interfaces and the results are fitted with Equations (7)–(9) and reported in Table 3.

Table 3. Stress-relaxation parameters.

Sample	E_d , mN/m	η_d , mN/(ms)	τ , s	β , -
P	27.0 ± 2.0 ^a	22 ± 1 ^a	43.0 ± 2.0 ^a	0.38 ± 0.02 ^a
PTG	21.0 ± 3.0 ^a	13 ± 2 ^b	34.1 ± 0.2 ^b	0.21 ± 0.02 ^b

Different letters in the same column refer to significantly different values. τ is the average relaxation time and β is the spreading of relation times; E_d is the dilatational effective surface elasticity, η_d the dilatational viscosity.

The interfacial film of the PTG solution shows lower elasticity and viscosity, a lower relaxation time value, and also a β coefficient lower than the untreated system. A lower relaxation time indicates a less structured interface, while the β coefficient is related to the distribution of the relaxation times. The lower the value compared to the unity, the wider the distribution of relaxation times, which is related to the different times required for the relaxation of the different protein fractions migrating to the interface [7]. Furthermore, a comparison with our previous work on soy proteins [7] revealed very similar behavior in terms of both the β coefficient (a measure of interfacial elasticity) and the elastic modulus. However, the relaxation time for the pea protein interface is lower. This effect is likely related to the prevalence of small protein fractions (2S) at the interface, which facilitate a faster relaxation process as reported in the literature [10]. Additionally, the expansion viscosity of the formed pea protein films is significantly higher than that observed with other vegetable proteins (hemp, soybean, and rice). This indicates a more rigid interface that is more resistant to structural relaxation [7].

Interfacial shear analysis was performed by a magnetic needle rheometer in oscillating mode and linear region. Figure 5 shows the data in terms of complex shear modulus (G_s^*) and phase angle (δ_s) for both sample P and PTG. Plots show very clearly that the interface

in the presence of TG results in an important decrease in the value of G_s^* and an increase in the delta angle. The TG addition changes the interfacial film from consistent and solid-like to weak and less elastic, in agreement with the results obtained by dilatational analysis.

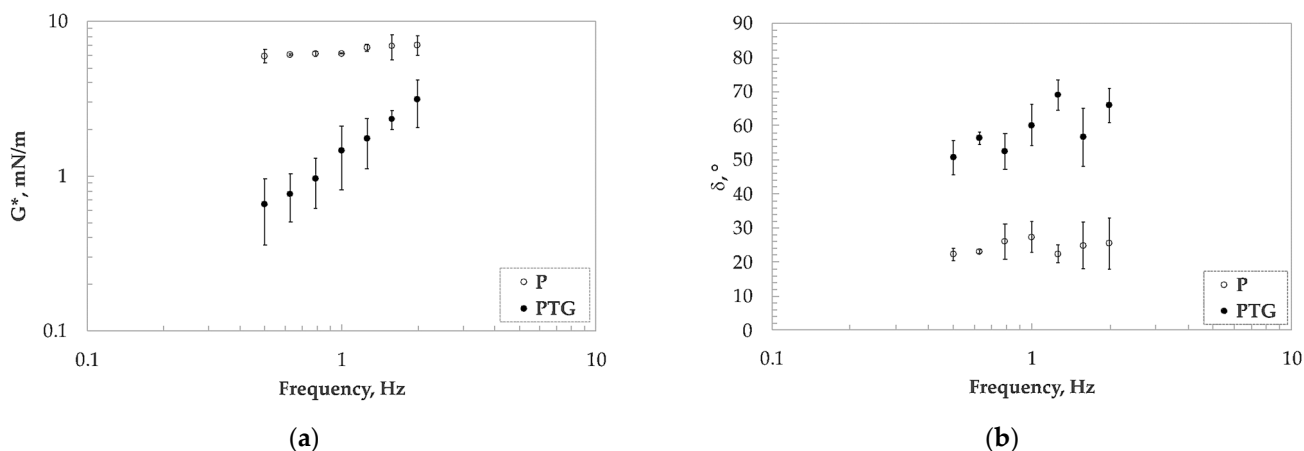


Figure 5. Surface shear complex modulus (a) and phase angle (b) for samples at 1% *w/w* of pea protein at 3 h of aging.

The results were interpreted by the power law model and the parameters are reported in Table 2. The PTG solution shows a weaker trend than the P sample in terms of both consistency and film structuring. In particular, the k_s parameter is significantly lower for the PTG sample, and the parameter n_s is higher, indicating an interfacial film with a low degree of structuring. The interface obtained by enzymatic treatment is less stable and weaker compared with the untreated one.

3.4. Bulk Shear Viscosity

Finally, viscosity tests were performed for the P solution with only pea protein and for the enzyme-treated solution (PTG). As can be seen from Figure 6, the two samples have two different behaviors. The sample with only pea protein shows a lower bulk viscosity than the enzymatically treated sample and also behaves like a purely viscous fluid. In fact, the viscosity of the P solution does not vary in the investigated shear rate range, so it behaves like a Newtonian material. On the contrary, the sample treated with TG shows a trend dependent on the deformation rate, typical of a shear-thinning material, and also higher viscosity values when compared to the P solution.

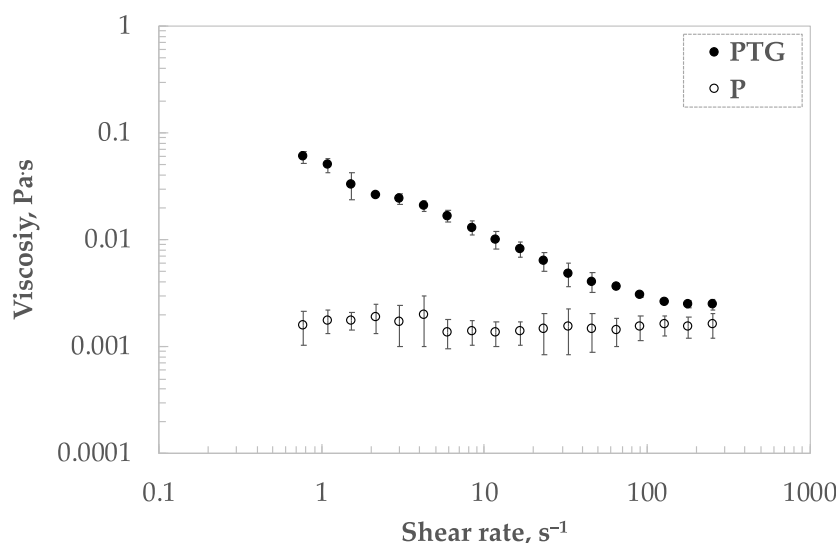


Figure 6. Shear bulk viscosity of P and PTG samples.

The results confirm the enzyme effect and agree with literature that suggests a crosslinking effect of TG in the presence of proteins rich in lysine, like pea proteins. The addition of TG, promoting crosslinking, increases the viscosity of the solution and has a gelling effect [49–52]. In fact, in many food systems, the TG enzyme is added to create more consistent and structured bulk systems [24,53–55].

4. Conclusions

This study investigated the effect of enzymatic modification with transglutaminase (TG) on the interfacial and bulk properties of pea protein isolate (PPI). The results showed that both untreated and TG-treated PPI exhibit good interfacial activity, similar to other vegetable proteins commonly used in the food industry.

The dynamic analysis both in dilatation and shear kinematics shows differences in the mechanical behavior of the interfaces. In particular, the sample with TG has an interface that is more consistent but with a lower structure than the interface of pure pea protein. From the stress relaxation data, it is possible to say that the interfacial film obtained with enzymatic treatment leads, moreover, to a less resistant interface above all because of the lower viscosity and relaxation time. Moreover, the shear analysis suggests that PTG has poor long-term stabilization capacity compared with the P solution due to the weakening of the interfacial film.

Finally, because of the well-known gelling properties of the lysine rich protein treatment with transglutaminase, the bulk shear viscosity was determined, confirming the crosslinking by TG, which results in a higher value of the bulk shear viscosity of the PTG and is coupled with a change in shear behavior from Newtonian, for the untreated protein, to shear thinning.

Author Contributions: Conceptualization, N.B. and D.G.; methodology, O.M.; software, M.F.O.P.; validation, O.M. and F.R.L.; formal analysis, M.F.O.P.; investigation, M.F.O.P. and O.M.; resources, N.B.; data curation, N.B., F.R.L. and D.G.; writing—original draft preparation, N.B. and O.M.; supervision, D.G. All authors have read and agreed to the published version of the manuscript.

Funding: This research received no external funding.

Data Availability Statement: The data presented in this study are available on request from the corresponding author.

Acknowledgments: The authors are grateful to the project “Next Generation EU—Technologies for climate change adaptation and quality of life improvement—Tech4You”.

Conflicts of Interest: The authors declare no conflicts of interest.

References

1. Golovinskaia, O.; Wang, C.-K. The hypoglycemic potential of phenolics from functional foods and their mechanisms. *Food Sci. Hum. Wellness* **2023**, *12*, 986–1007. [[CrossRef](#)]
2. Bauer-Estrada, K.; Sandoval-Cuellar, C.; Rojas-Muñoz, Y.; Quintanilla-Carvajal, M.X. The modulatory effect of encapsulated bioactives and probiotics on gut microbiota: Improving health status through functional food. *Food Funct.* **2023**, *14*, 32–55. [[CrossRef](#)] [[PubMed](#)]
3. Kaur, S.; Das, M. Functional foods: An overview. *Food Sci. Biotechnol.* **2011**, *20*, 861–875. [[CrossRef](#)]
4. Baldino, N.; Carnevale, I.; Laitano, F.; Lupi, F.R.; Curcio, S.; Gabriele, D. Formulation of bread model doughs with resistant starch, vegetable proteins and transglutaminase. *Eur. Food Res. Technol.* **2020**, *246*, 397–408. [[CrossRef](#)]
5. Kaczynska, K.; Wouters, A.G.; Delcour, J.A. Microbial transglutaminase induced modification of wheat gliadin based nanoparticles and its impact on their air-water interfacial properties. *Food Hydrocoll.* **2022**, *127*, 107471. [[CrossRef](#)]
6. Lu, S.; Xiong, W.; Yao, Y.; Zhang, J.; Wang, L. Investigating the physicochemical properties and air-water interface adsorption behavior of transglutaminase-crosslinking rapeseed protein isolate. *Food Res. Int.* **2023**, *174*, 113505. [[CrossRef](#)] [[PubMed](#)]
7. Mileti, O.; Baldino, N.; Carmona, J.A.; Lupi, F.R.; Muñoz, J.; Gabriele, D. Shear and dilatational rheological properties of vegetable proteins at the air/water interface. *Food Hydrocoll.* **2022**, *126*, 107472. [[CrossRef](#)]
8. Mastromatteo, M.; Danza, A.; Guida, M.; Del Nobile, M.A. Formulation optimisation of vegetable flour-loaded functional bread Part I: Screening of vegetable flours and structuring agents. *Int. J. Food Sci. Technol.* **2012**, *47*, 1313–1320. [[CrossRef](#)]
9. Shen, Q.; Zheng, W.; Han, F.; Zuo, J.; Dai, J.; Tang, C.; Song, R.; Li, B.; Chen, Y. Air-water interfacial properties and quantitative description of pea protein isolate-Tween 20. *Food Hydrocoll.* **2023**, *139*, 108568. [[CrossRef](#)]

10. Shen, Q.; Li, J.; Shen, X.; Zhu, X.; Dai, J.; Tang, C.; Song, R.; Li, B.; Chen, Y. Linear and nonlinear interface rheological behaviors and structural properties of pea protein (vicilin, legumin, albumin). *Food Hydrocoll.* **2023**, *139*, 108500. [[CrossRef](#)]
11. Liang, H.-N.; Tang, C.-H. pH-dependent emulsifying properties of pea [*Pisum sativum* (L.)] proteins. *Food Hydrocoll.* **2013**, *33*, 309–319. [[CrossRef](#)]
12. A Rubio, L.; Pérez, A.; Ruiz, R.; Guzmán, M.A.; Aranda-Olmedo, I.; Clemente, A. Characterization of pea (*Pisum sativum*) seed protein fractions. *J. Sci. Food Agric.* **2014**, *94*, 280–287. [[CrossRef](#)]
13. Shen, Q.; Luo, Y.; Zheng, W.; Xiong, T.; Han, F.; Zuo, J.; Dai, J.; Li, B.; Chen, Y. Nonlinear rheological behavior and quantitative proteomic analysis of pea protein isolates at the air-water interface. *Food Hydrocoll.* **2023**, *135*, 108115. [[CrossRef](#)]
14. Sharif, H.R.; Williams, P.A.; Sharif, M.K.; Abbas, S.; Majeed, H.; Masamba, K.G.; Safdar, W.; Zhong, F. Current progress in the utilization of native and modified legume proteins as emulsifiers and encapsulants—A review. *Food Hydrocoll.* **2018**, *76*, 2–16. [[CrossRef](#)]
15. Yang, J.; Zamani, S.; Liang, L.; Chen, L. Extraction methods significantly impact pea protein composition, structure and gelling properties. *Food Hydrocoll.* **2021**, *117*, 106678. [[CrossRef](#)]
16. Gao, Z.; Shen, P.; Lan, Y.; Cui, L.; Ohm, J.-B.; Chen, B.; Rao, J. Effect of alkaline extraction pH on structure properties, solubility, and beany flavor of yellow pea protein isolate. *Food Res. Int.* **2020**, *131*, 109045. [[CrossRef](#)] [[PubMed](#)]
17. Stone, A.K.; Karalash, A.; Tyler, R.T.; Warkentin, T.D.; Nickerson, M.T. Functional attributes of pea protein isolates prepared using different extraction methods and cultivars. *Food Res. Int.* **2015**, *76*, 31–38. [[CrossRef](#)]
18. Tanger, C.; Engel, J.; Kulozik, U. Influence of extraction conditions on the conformational alteration of pea protein extracted from pea flour. *Food Hydrocoll.* **2020**, *107*, 105949. [[CrossRef](#)]
19. Savoca, M.P.; Tonoli, E.; Atobatele, A.G.; Verderio, E.A.M. Biocatalysis by Transglutaminases: A Review of Biotechnological Applications. *Micromachines* **2018**, *9*, 562. [[CrossRef](#)]
20. Partanen, R.; Paananen, A.; Forssell, P.; Linder, M.B.; Lille, M.; Buchert, J.; Lantto, R. Effect of transglutaminase-induced cross-linking of sodium caseinate on the properties of equilibrated interfaces and foams. *Colloids Surfaces A Physicochem. Eng. Asp.* **2009**, *344*, 79–85. [[CrossRef](#)]
21. Tamm, F.; Drusch, S. Impact of enzymatic hydrolysis on the interfacial rheology of whey protein/pectin interfacial layers at the oil/water-interface. *Food Hydrocoll.* **2017**, *63*, 8–18. [[CrossRef](#)]
22. Zhang, M.; Zhang, B.-Y.; Sun, X.; Liu, Y.-A.; Yu, Z.; Wang, X.; Xu, N. Freeze-thaw stability of transglutaminase-induced soy protein-maltose emulsion gel: Focusing on morphology, texture properties, and rheological characteristics. *Int. J. Biol. Macromol.* **2024**, *261*, 129716. [[CrossRef](#)] [[PubMed](#)]
23. Dong, C.; Zhao, J.; Wang, L.; Jiang, J. Modified pea protein coupled with transglutaminase reduces phosphate usage in low salt myofibrillar gel. *Food Hydrocoll.* **2023**, *139*, 108577. [[CrossRef](#)]
24. Moreno, H.M.; Tovar, C.A.; Domínguez-Timón, F.; Cano-Báez, J.; Díaz, M.T.; Pedrosa, M.M.; Borderías, A.J. Gelation of commercial pea protein isolate: Effect of microbial transglutaminase and thermal processing. *Food Sci. Technol.* **2020**, *40*, 800–809. [[CrossRef](#)]
25. Shand, P.; Ya, H.; Pietrasik, Z.; Wanasundara, P. Transglutaminase treatment of pea proteins: Effect on physicochemical and rheological properties of heat-induced protein gels. *Food Chem.* **2008**, *107*, 692–699. [[CrossRef](#)]
26. Romero, A.; Beaumal, V.; David-Briand, E.; Cordobes, F.; Guerrero, A.; Anton, M. Interfacial and emulsifying behaviour of rice protein concentrate. *Food Hydrocoll.* **2012**, *29*, 1–8. [[CrossRef](#)]
27. Seta, L.; Baldino, N.; Gabriele, D.; Lupi, F.R.; de Cindio, B. The effect of surfactant type on the rheology of ovalbumin layers at the air/water and oil/water interfaces. *Food Hydrocoll.* **2012**, *29*, 247–257. [[CrossRef](#)]
28. Seta, L.; Baldino, N.; Gabriele, D.; Lupi, F.R.; de Cindio, B. The influence of carrageenan on interfacial properties and short-term stability of milk whey proteins emulsions. *Food Hydrocoll.* **2013**, *32*, 373–382. [[CrossRef](#)]
29. Wüstneck, R.; Enders, P.; Ebisch, T.; Miller, R. Axiallysymmetric stress relaxation and surface dilation rheology of docosanic acid monolayers spread at the interface of pendant drops in the short time region. *Thin Solid Films* **1997**, *298*, 39–46. [[CrossRef](#)]
30. Ward, A.F.H.; Tordai, L. Time-Dependence of Boundary Tensions of Solutions I. The Role of Diffusion in Time-Effects. *J. Chem. Phys.* **1946**, *14*, 453–461. [[CrossRef](#)]
31. Mileti, O.; Baldino, N.; Lupi, F.R.; Gabriele, D. Interfacial behavior of vegetable protein isolates at sunflower oil/water interface. *Colloids Surf. B Biointerfaces* **2023**, *221*, 113035. [[CrossRef](#)] [[PubMed](#)]
32. Saulnier, P.; Boury, F.; Malzert, A.; Heurtault, B.; Ivanova, T.; Cagna, A.; Panaïotov, I.; Proust, J.E. Rheological Model for the Study of Dilational Properties of Monolayers. Comportment of Dipalmitoylphosphatidylcholine (DPPC) at the Dichloromethane (DCM)/Water Interface under Ramp Type or Sinusoidal Perturbations. *Langmuir* **2001**, *17*, 8104–8111. [[CrossRef](#)]
33. Ivanov, I.B.; Danov, K.D.; Ananthapadmanabhan, K.P.; Lips, A. Interfacial rheology of adsorbed layers with surface reaction: On the origin of the dilatational surface viscosity. *Adv. Colloid Interface Sci.* **2005**, *114–115*, 61–92. [[CrossRef](#)] [[PubMed](#)]
34. Doan, C.D.; Ghosh, S. Formation and Stability of Pea Proteins Nanoparticles Using Ethanol-Induced Desolvation. *Nanomaterials* **2019**, *9*, 949. [[CrossRef](#)]
35. Barac, M.; Cabrilo, S.; Pesic, M.; Stanojevic, S.; Zilic, S.; Macej, O.; Ristic, N. Profile and Functional Properties of Seed Proteins from Six Pea (*Pisum sativum*) Genotypes. *Int. J. Mol. Sci.* **2010**, *11*, 4973–4990. [[CrossRef](#)]
36. Tang, C.-H.; Ten, Z.; Wang, X.-S.; Yang, X.-Q. Physicochemical and Functional Properties of Hemp (*Cannabis sativa* L.) Protein Isolate. *J. Agric. Food Chem.* **2006**, *54*, 8945–8950. [[CrossRef](#)] [[PubMed](#)]

37. XCao, X.; Wen, H.; Li, C.; Gu, Z. Differences in functional properties and biochemical characteristics of congenetic rice proteins. *J. Cereal Sci.* **2009**, *50*, 184–189. [[CrossRef](#)]
38. Karaca, A.C.; Low, N.; Nickerson, M. Emulsifying properties of chickpea, faba bean, lentil and pea proteins produced by isoelectric precipitation and salt extraction. *Food Res. Int.* **2011**, *44*, 2742–2750. [[CrossRef](#)]
39. Sejersen, M.T.; Salomonsen, T.; Ipsen, R.; Clark, R.; Rolin, C.; Engelsen, S.B. Zeta potential of pectin-stabilised casein aggregates in acidified milk drinks. *Int. Dairy J.* **2007**, *17*, 302–307. [[CrossRef](#)]
40. Rodrigueznino, M.; Sánchez, C.C.; Ruizhenestrosa, V.; Patino, J.M.R. Milk and soy protein films at the air–water interface. *Food Hydrocoll.* **2005**, *19*, 417–428. [[CrossRef](#)]
41. Martin, A.; Bos, M.; van Vliet, T. Interfacial rheological properties and conformational aspects of soy glycinin at the air/water interface. *Food Hydrocoll.* **2002**, *16*, 63–71. [[CrossRef](#)]
42. Mileti, O.; Baldino, N.; Luzzi, S.; Lupi, F.R.; Gabriele, D. Interfacial Rheological Study of β -Casein/Pectin Mixtures at the Air/Water Interface. *Gels* **2024**, *10*, 41. [[CrossRef](#)] [[PubMed](#)]
43. Patino, J.M.R.; Pilosof, A.M. Protein–polysaccharide interactions at fluid interfaces. *Food Hydrocoll.* **2011**, *25*, 1925–1937. [[CrossRef](#)]
44. Camino, N.A.; Pérez, O.E.; Sanchez, C.C.; Patino, J.M.R.; Pilosof, A.M. Hydroxypropylmethylcellulose surface activity at equilibrium and adsorption dynamics at the air–water and oil–water interfaces. *Food Hydrocoll.* **2009**, *23*, 2359–2368. [[CrossRef](#)]
45. Pérez, O.E.; Sánchez, C.C.; Pilosof, A.M.; Patino, J.M.R. Kinetics of adsorption of whey proteins and hydroxypropyl-methylcellulose mixtures at the air–water interface. *J. Colloid Interface Sci.* **2009**, *336*, 485–496. [[CrossRef](#)] [[PubMed](#)]
46. Perez, A.A.; Carrara, C.R.; Sánchez, C.C.; Santiago, L.G.; Patino, J.M.R. Interfacial dynamic properties of whey protein concentrate/polysaccharide mixtures at neutral pH. *Food Hydrocoll.* **2009**, *23*, 1253–1262. [[CrossRef](#)]
47. Færgemand, M.; Murray, B.S.; Dickinson, E. Cross-Linking of Milk Proteins with Transglutaminase at the Oil–Water Interface. *J. Agric. Food Chem.* **1997**, *45*, 2514–2519. [[CrossRef](#)]
48. Bergfreund, J.; Bertsch, P.; Fischer, P. Effect of the hydrophobic phase on interfacial phenomena of surfactants, proteins, and particles at fluid interfaces. *Curr. Opin. Colloid Interface Sci.* **2021**, *56*, 101509. [[CrossRef](#)]
49. Sun, X.D.; Arntfield, S.D. Gelation properties of myofibrillar/pea protein mixtures induced by transglutaminase crosslinking. *Food Hydrocoll.* **2012**, *27*, 394–400. [[CrossRef](#)]
50. Tanimoto, S.Y.; Kinsella, J.E. Enzymic modification of proteins: Effects of transglutaminase cross-linking on some physical properties of .beta.-lactoglobulin. *J. Agric. Food Chem.* **1988**, *36*, 281–285. [[CrossRef](#)]
51. Shen, Y.; Hong, S.; Singh, G.; Koppel, K.; Li, Y. Improving functional properties of pea protein through “green” modifications using enzymes and polysaccharides. *Food Chem.* **2022**, *385*, 132687. [[CrossRef](#)] [[PubMed](#)]
52. Dickinson, E. Enzymic crosslinking as a tool for food colloid rheology control and interfacial stabilization. *Trends Food Sci. Technol.* **1997**, *8*, 334–339. [[CrossRef](#)]
53. Bönisch, M.P.; Huss, M.; Weitzl, K.; Kulozik, U. Transglutaminase cross-linking of milk proteins and impact on yoghurt gel properties. *Int. Dairy J.* **2007**, *17*, 1360–1371. [[CrossRef](#)]
54. Yaputri, B.P.; Feyzi, S.; Ismail, B.P. Transglutaminase-Induced Polymerization of Pea and Chickpea Protein to Enhance Functionality. *Gels* **2023**, *10*, 11. [[CrossRef](#)]
55. Qin, J.; Zhao, Y.; Zhou, J.; Zhang, G.; Li, J.; Liu, X. Rheological properties of transglutaminase-treated concentrated pea protein under conditions relevant to high-moisture extrusion processing. *Front. Nutr.* **2022**, *9*, 970010. [[CrossRef](#)]

Disclaimer/Publisher’s Note: The statements, opinions and data contained in all publications are solely those of the individual author(s) and contributor(s) and not of MDPI and/or the editor(s). MDPI and/or the editor(s) disclaim responsibility for any injury to people or property resulting from any ideas, methods, instructions or products referred to in the content.